doi:10.1093/brain/awx232 BRAIN 2017: 140; 3023–3038 | 3023

BRAIN
A JOURNAL OF NEUROLOGY

Chemogenetic locus coeruleus activation restores reversal learning in a rat model of Alzheimer's disease

Jacki M. Rorabaugh,[1] Termpanit Chalermpalanupap,[1] Christian A. Botz-Zapp,[1] Vanessa M. Fu,[1] Natalie A. Lembeck,[1] Robert M. Cohen[2] and David Weinshenker[1]

See Grinberg and Heinsen (doi:10.1093/brain/awx261) for a scientific commentary on this article.

Clinical evidence suggests that aberrant tau accumulation in the locus coeruleus and noradrenergic dysfunction may be a critical early step in Alzheimer's disease progression. Yet, an accurate preclinical model of these phenotypes that includes early pretangle tau accrual in the locus coeruleus, loss of locus coeruleus innervation and deficits locus coeruleus/norepinephrine modulated behaviours, does not exist, hampering the identification of underlying mechanisms and the development of locus coeruleus-based therapies. Here, a transgenic rat (TgF344-AD) expressing disease-causing mutant amyloid precursor protein (APP_{sw}) and presenilin-1 (PS1ΔE9) was characterized for histological and behavioural signs of locus coeruleus dysfunction reminiscent of mild cognitive impairment/early Alzheimer's disease. In TgF344-AD rats, hyperphosphorylated tau was detected in the locus coeruleus prior to accrual in the medial entorhinal cortex or hippocampus, and tau pathology in the locus coeruleus was negatively correlated with noradrenergic innervation in the medial entorhinal cortex. Likewise, TgF344-AD rats displayed progressive loss of hippocampal norepinephrine levels and locus coeruleus fibres in the medial entorhinal cortex and dentate gyrus, with no frank noradrenergic cell body loss. Cultured mouse locus coeruleus neurons expressing hyperphosphorylation-prone mutant human tau had shorter neurites than control neurons, but similar cell viability, suggesting a causal link between pretangle tau accrual and altered locus coeruleus fibre morphology. TgF344-AD rats had impaired reversal learning in the Morris water maze compared to their wild-type littermates, which was rescued by chemogenetic locus coeruleus activation via designer receptors exclusively activated by designer drugs (DREADDs). Our results indicate that TgF344-AD rats uniquely meet several key criteria for a suitable model of locus coeruleus pathology and dysfunction early in Alzheimer's disease progression, and suggest that a substantial window of opportunity for locus coeruleus/ norepinephrine-based therapeutics exists.

1 Department of Human Genetics, Emory University School of Medicine, Atlanta GA 30322, USA
2 Departments of Psychiatry and Behavioral Sciences, Emory University School of Medicine, Atlanta GA 30322, USA

Correspondence to: David Weinshenker
Department of Human Genetics, Emory University School of Medicine, Atlanta GA 30322, USA
E-mail: dweinsh@emory.edu

Keywords: Alzheimer's disease; locus coeruleus; norepinephrine; TgF344-AD; DREADD

Abbreviations: CNO = clozapine N-oxide; DREADD = designer receptors exclusively activated by designer drugs; DBH = dopamine β-hydroxylase; mEC = medial entorhinal cortex; mPFC = medial prefrontal cortex; MHPG = 3-methoxy-4-hydroxyphenylglycol

Received March 18, 2017. Revised July 14, 2017. Accepted July 18, 2017. Advance Access publication September 25, 2017

Introduction

Alzheimer's disease, which is characterized by amyloid-β plaques and tau neurofibrillary tangles, is the most prevalent form of dementia in the USA (Alzheimer's Association, 2016). Current therapies for Alzheimer's disease provide marginal symptomatic relief and do not retard disease progression. Although research efforts have enhanced understanding of disease mechanisms, efforts to treat Alzheimer's disease have failed, potentially because of irreversible neuron loss that occurs once cognitive impairment arises. As such, current research is focused on early detection and therapeutic intervention.

It has been appreciated for some time that the locus coeruleus, the major noradrenergic nucleus in the brain, degenerates in Alzheimer's disease (Tomlinson *et al.*, 1981; Haglund *et al.*, 2006; Weinshenker, 2008). At the time of clinical diagnosis (i.e. mild cognitive impairment/early Alzheimer's disease) significant loss of forebrain norepinephrine and locus coeruleus fibres is evident, followed by frank cell body degeneration in mid- to advanced stage disease (Braak and Del Tredici, 2012; Mather and Harley, 2016). Cell loss in the locus coeruleus is a better predictor of cognitive symptoms than degeneration in other brain regions affected by Alzheimer's disease, including the medial entorhinal cortex (mEC), hippocampus, and nucleus basalis of Meynert (Wilson *et al.*, 2013; Kelly *et al.*, 2017). More recent studies indicate that hyperphosphorylated tau in the locus coeruleus is among the first detectable Alzheimer's disease pathologies in post-mortem human brains, appearing before tau pathology in the mEC and often decades prior to cognitive symptoms (Braak *et al.*, 2011; Andres-Benito *et al.*, 2017; Ehrenberg *et al.*, 2017).

The locus coeruleus is the major source of norepinephrine in the forebrain and is critical for attention, arousal and specific aspects of learning and memory (Sara, 2009; Aston-Jones and Cohen, 2014). High locus coeruleus neuron density protects against cognitive decline during ageing, while tangle burden in the locus coeruleus is correlated with cognitive decline (Wilson *et al.*, 2013; Kelly *et al.*, 2017). In addition, norepinephrine has potent anti-inflammatory properties and promotes amyloid-β clearance (Chalermpalanupap *et al.*, 2013; Heneka *et al.*, 2015; Feinstein *et al.*, 2016). Thus, it is not surprising that lesioning the locus coeruleus or genetically reducing norepinephrine levels exacerbates Alzheimer's disease-like pathology, neuroinflammation, and/or cognitive impairment in amyloid-based transgenic mouse models (Heneka *et al.*, 2002; Heneka, 2006; Jardanhazi-Kurutz *et al.*, 2010; Kalinin *et al.*, 2012; Hammerschmidt *et al.*, 2013; Kummer *et al.*, 2014). While this work demonstrates that inducing locus coeruleus degeneration worsens Alzheimer's disease pathology, it recapitulates the frank degeneration of locus coeruleus neurons that is not observed until mid-stage Alzheimer's disease (~Braak stage III–IV), a time when pharmaceutical interventions have failed (Kelly *et al.*, 2017; Theofilas *et al.*, 2017). Moreover, amyloid precursor protein (APP) transgenic mice do not recapitulate the tau pathology observed in humans, potentially because endogenous mouse tau is resistant to aggregation (Morrissette *et al.*, 2009; Woerman *et al.*, 2016). Mice ubiquitously expressing mutant human tau do develop pathology, but not 'endogenous' pretangle tau or neurofibrillary tangles, and they are considered models of tauopathy rather than Alzheimer's disease (Morrissette *et al.*, 2009). An animal model that recapitulates early locus coeruleus tau pathology and dysfunction, prior to cell body degeneration, may provide valuable insights into early disease mechanisms and potential locus coeruleus-based therapies.

Compared to mice, rat tau is more similar to human tau, and perhaps as a result, amyloid-based transgenic rats display unique phenotypes such as conversion of endogenous rat tau into hyperphosphorylated forms (Cohen *et al.*, 2013; Do Carmo and Cuello, 2013). The TgF344-AD rat expresses disease-causing mutant human APP (*APPsw*) and presenilin 1 (*PS1ΔE9*), and displays canonical amyloid plaques as well as core components of Alzheimer's disease that are often missing in transgenic mice, including age-dependent cognitive impairment, amyloid-β oligomers, gliosis and apoptotic neuronal loss in the forebrain (Cohen *et al.*, 2013). Notably, TgF344-AD rats do not express a human tau transgene but display age-dependent endogenous hyperphosphorylated tau in the hippocampus and medial prefrontal cortex (mPFC). Based on these features, we reasoned that the TgF344-AD rat model might be a good candidate to accurately recapitulate locus coeruleus pathology and dysfunction in mild cognitive impairment/early Alzheimer's disease, and established that such a model would need to encompass the following features: (i) age-dependent hyperphosphorylated tau accumulation in the locus coeruleus prior to other brain regions; (ii) no locus coeruleus cell body loss; (iii) norepinephrine and/or noradrenergic fibre deficiency in locus coeruleus target regions; and (iv) impairment in locus coeruleus/norepinephrine-modulated behaviours. Moreover, if increasing locus coeruleus/norepinephrine activity restores memory, this would add basic science backing to the mounting clinical evidence suggesting that adrenergic-based therapies could be effective early in Alzheimer's disease. Stimulatory designer receptors exclusively activated by designer drugs (DREADDs) can be expressed in locus coeruleus neurons via viral vectors harbouring the PRSx8 locus coeruleus-specific promotor. This system allows for long-lasting locus coeruleus neuron activation following administration of the DREADD ligand, clozapine N-oxide (CNO) (Vazey and Aston-Jones, 2014; Fortress *et al.*, 2015). In this study, we characterized locus coeruleus pathology and dysfunction in the TgF344-AD rat, compared it to the pathology in the hippocampus and mEC, and then investigated whether increasing locus coeruleus activity with DREADDs could reverse cognitive impairment in these animals.

Materials and methods

Animals

TgF344-AD rats heterozygous for an *APPsw/PS1ΔE9* transgene and wild-type littermates were housed and maintained in the animal facility at Emory University. All procedures were performed under IACUC compliance. No sex differences in Alzheimer's disease-like pathology or behaviour have been reported for these rats, and thus roughly equal numbers of males and females were used for all studies (Cohen *et al.*, 2013). Rats were pair-housed on a 12-h light/dark cycle and given *ad libitum* access to food and chow except during behavioural testing.

Tissue preparation

At 6 or 16 months, rats were anaesthetized with ketamine [100 mg/kg; intraperitoneally (i.p.); Henry Schein] and xylazine (20 mg/kg i.p., Patterson Veterinary Supply) and perfused with ice cold potassium phosphate-buffered saline (PBS) followed by 4% paraformaldehyde. Brains were removed and paraffin-embedded (6 months: wild-type $n = 3$ male, 2 female and TgF344-AD $n = 3$ male, 2 female; 16 months: wild-type $n = 3$ male, 2 female and TgF344-AD $n = 3$ male, 2 female) or immersed in 30% sucrose (6 months: wild-type $n = 2$ male, 4 female and TgF344-AD $n = 2$ male, 4 female; 16 months: wild-type $n = 6$ male, 2 female and TgF344-AD $n = 6$ male, 2 female) and sectioned at the level of the locus coeruleus (−8.8 to 10.5 mm from bregma), mEC (−7.0 to −8.0 mm), dorsal hippocampus (−1.8 to −3.6 mm), paraventricular nucleus of the thalamus (PVT) (−1.8 to −3.6 mm) and mPFC (4.2 to 2.2 mm).

Immunohistochemistry

Paraffin-embedded tissue

Slides containing locus coeruleus, mEC and hippocampus sections were deparaffinized and immunostained using CP13 Ser205 phospho-antibody (1:2000, gifted from Peter Davies), PHF-1 Ser396/Ser404 phospho-antibody (1:1000, gifted from Peter Davies), or MC1 conformational antibody against amino acids 7–9 and 313–322 (1:1000, gifted from Peter Davies) and biotinylated goat anti-mouse secondary antibody (1:500; Vector Labs), followed by avidin-biotin complex (ABC; Vector Labs) and 3,3'-diaminobenzidine (Sigma-Aldrich) as previously described (Turnbull and Coulson, 2017). All tau stains were processed with positive controls (hippocampus from patients with Alzheimer's disease, hippocampus of P301S tau transgenic mice) and technical negative controls (no primary antibody) to ensure specificity of staining. A second set of mEC slides was stained for amyloid-β or the norepinephrine transporter (NET) with 10 min pretreatment in 80% formic acid, followed by 10 min incubation in a 0.3 N sodium hydroxide, 0.9% hydrogen peroxide solution, a block in 10% normal donkey serum with 0.05% Tween-20 and overnight incubation with the 4G8 antibody (1:1000, Convance) or a mouse anti-NET antibody (1:1000, NET05-2; MAb Technologies). The next day, slides were incubated with donkey anti-mouse Alexa Fluor® 488 (1:600; A-21202, Life Technologies) and coverslipped. Another set of locus coeruleus containing slides was stained with rabbit anti-GFAP (1:1000; 019-19741, Wako Pure Chemical Industries) or ThioS and mouse anti-tyrosine hydroxylase (TH; 1:1000; 22941, Immunostar) primary antibodies and donkey anti-rabbit Alexa Fluor® 568 (1:600; A10048, Life Technologies) and donkey anti-mouse Alexa Fluor® 488 (1:600; A-21202, Life Technologies) secondary antibodies, and counterstained with Neurotrace 640/660 (N21438, Life Technologies).

Free-floating tissue

Sections from locus coeruleus, dorsal hippocampus, mPFC, and PVT were stained as previously described with rabbit anti-Iba-1 (1:1000) and mouse anti-TH or anti-dopamine β-hydroxylase (DBH; 1:1000; MAB308, Millipore), respectively. Sections were incubated with the corresponding donkey anti-rabbit A568 or anti-mouse A488 secondary antibodies. Locus coeruleus tissue from DREADD-expressing rats (see 'Morris water maze' section for details) was stained with rabbit anti-TH (1:5000; 40101-0, PelFreeze) or rabbit anti-c-Fos (1:1000, sc-52, Santa Cruz Biotech) and mouse anti-haemagglutinin (HA; 1:1000; MMS-101P, Biolegend) primary antibodies and incubated with the aforementioned fluorescent secondary antibodies.

A separate set of sections was used for locus coeruleus stereology studies. Every third locus coeruleus (−10.5 to −8.8 mm from bregma) section was incubated for 30 min in 1% hydrogen peroxide in PBS, blocked for 30 min in 5% normal goat serum in PBS and then incubated overnight in rabbit anti-TH primary antibody (1:10 000) in 2% normal goat serum, PBS-Tris solution at 4°C. Next, sections were incubated for 60 min in biotinylated goat anti-rabbit secondary (1:600; BA-1000, Vector Labs), followed by ABC solution for 60 min and then 3,3'-diaminobenzidine.

Image analysis

For each rat, two to three brain sections were analysed and averaged together to determine group means. All image analysis was performed with ImageJ software for background subtraction, threshold application (Otsu method) and quantification ($CP13^+$, TH^+, $Iba1^+$, $GFAP^+$ and $c\text{-}Fos^+$) based on size and shape criteria for neurons (75–100 μm^2; circularity 0.3–1.0), glia (50–1000 μm^2, circularity 0.15–10) and nuclei (30–70 μm^2, circularity 0.5–1.0), as well as overlap with TH^+ or HA^+ cells where appropriate. Line scan analysis was performed to determine DBH^+/NET^+ fibre density in mEC, hippocampus, mPFC, and PVT as previously described (Sathyanesan *et al.*, 2012). Experimenter was blind to genotype during image collection and analysis.

Unbiased stereology

Stereology was performed using MBF StereoInvestigator software and a Zeiss microscope utilizing the optical fractionator probe and systematic analysis of randomly placed counting frames (size, 75 × 50 μm) on a counting grid (size of 100 × 100 μm) and sampled (20 μm optical dissector with 2 μm upper and lower guard zones) to obtain unbiased counts of TH^+ neurons. The nucleator probe (six rays) was used to measure cell size. Experimenter was blind to genotype, and all locus coeruleus counts had a Gundersen coefficient

(m = 1) of <0.10 to ensure accuracy and consistency (Gundersen *et al.*, 1999).

Tissue catecholamine analysis

At 6 months (wild-type $n = 3$ male, 3 female; TgF344-AD $n = 4$ male, 2 female) and 16 months (wild-type $n = 4$ male, 4 female; TgF344-AD $n = 3$ male, 5 female), rats were euthanized with carbon dioxide and brains were rapidly removed. The hippocampus and mPFC were dissected out and frozen on dry ice. Samples were thawed, weighed, homogenized in 0.1 N perchloric acid (10× v/wt) and centrifuged (16 000*g*) for 30 min at 4°C. The supernatant was centrifuged through 0.45 µm filters (Fischer Scientific, 10-800-195) at 4000*g* for 10 min at 4°C. Monoamines were examined by high performance liquid chromatography (HPLC) with electrochemical detection as described previously (Song *et al.*, 2012). For HPLC, an ESA 5600A CoulArray detection system, equipped with an ESA Model 584 pump and an ESA 542 refrigerated autosampler was used. Separations were performed using an MD-150 × 3.2 mm C18 column at 30°C. The mobile phase consisted of 8% acetonitrile, 75 mM NaH_2PO_4, 1.7 mM 1-octanesulfonic acid sodium and 0.025% trimethylamine at pH 2.9. 20 µl of sample was injected, and the samples were eluted isocratically at 0.4 ml/min and detected using a 6210 electrochemical cell (ESA) equipped with 5020 guard cell. Guard cell potential was set at 475 mV, while analytical cell potentials were −175, 100, 350 and 425 mV. The analytes were identified by the matching criteria of retention time and sensor ratio measures to known standards (Sigma-Aldrich) consisting of norepinephrine and 4-hydroxy-3-methoxyphenylglycol (MHPG). Compounds were quantified by comparing peak areas to those of standards on the dominant sensor.

Primary neuron culture

Locus coeruleus neuron cultures were derived from post-natal Day 1 TH-GFP and TH-GFP/P301S tau transgenic mouse pups. Pups were decapitated and the locus coeruleus was dissected under a fluorescence microscope (MZ FLIII, Leica) in ice-cold Hank's balanced buffer with 1% penicillin/streptomycin (pen/strep; Lonza) and HEPES (Cellgro). Tissue was incubated for 30 min in 37°C plating media (33.3 mM glucose, 10% horse serum, 1% pen/strep in minimal essential medium, 11095-080, ThermoFisher Scientific) containing papain (1 mg/ml, P4762, Sigma-Aldrich), Dispase I (0.5 U/ml, 07923, StemCell Technologies) and DNase I (20 µg/ml, DN25, Sigma-Aldrich). Tissue was washed in plating media and dissociated by gentle trituration. Cells were plated on coverslips coated with poly-D-lysine and laminin (08-774-384, ThermoFisher Scientific) and incubated for 30 min at 37°C before wells were flooded with plating media. After 2 h, half of the media was replaced with Neurobasal® media (21103-049, ThermoFisher Scientific) supplemented with 1% pen/strep, B-27 (17504-044, ThermoFisher Scientific) and 2 mM L-glutamine (25-005-CI, Cellgro). The following day and every 3 days thereafter, half of the media was exchanged with media containing aphidicolin (1.0 µg/ml, A-1026; A.G Scientific). On *in vitro* Day 11, cells were fixed and stained for TH (1:1000) and human tau (1:500, HT7; MN1000, Abcam). Three images (×10) were taken from each coverslip and average neurite length was calculated using the NeuriteTracer plugin for ImageJ.

Stereotaxic injection of PRSx8-hM3Dq-HA virus

At 13.5 months of age, TgF344-AD ($n = 6$ male, 7 female) and wild-type ($n = 7$ male, 9 female) rats were anesthetized with isoflurane, pretreated with meloxicam (1 mg/kg; i.p.) and given bilateral stereotaxic injections (1.3 µl/side) of an adeno-associated virus (AAV) 2/9 containing a HA-hM3Dq plasmid (1.12×10^{13} genome copies/ml; initially provided by E. Vazey and G. Aston-Jones and subsequently purchased from the University of Pennsylvania Viral Vector Core) under the control of the locus coeruleus-specific PRSx8 promoter aimed at the locus coeruleus (AP: −9.3 mm, ML: ±1.3 mm; DV: −7.4 mm from bregma) (Vazey and Aston-Jones, 2014). Morris water maze testing began 6–8 weeks after virus injection surgery to allow sufficient time for robust viral expression. Although all rats received bilateral locus coeruleus injections, unilateral DREADD expression was observed in 80% of the animals, most likely due to difficulties targeting a deep brainstem nucleus of such small dimensions. The majority (5/6) of bilateral DREADD-expressing rats were treated with vehicle, and data from bilateral and unilateral expressing rats were pooled. Unilateral DREADD-induced stimulation of the locus coeruleus is sufficient for widespread brain activation patterns and behavioural effects; similar cortical activity and emergence from anaesthesia were reported in rats with unilateral or bilateral DREADD expression in the locus coeruleus (Vazey and Aston-Jones, 2014).

Morris water maze

The Morris water maze was performed in a cylindrical tank (183 cm × 91 cm) filled with opaque water obscuring a platform (water ~2 cm above platform height) located in the centre of a quadrant. Extra-maze visual cues were posted around the tank. An overhead camera and Topscan software (Cleversys, Reston, VA) were used to track movements including calculations of latency, distance travelled and average swim speed. Rats (6 month: wild-type $n = 2$ male, 4 female and TgF344-AD $n = 2$ male, 4 female; 16 month: wild-type $n = 6$ male and TgF344-AD $n = 6$ male) were handled for 3 days prior to the Morris water maze task. During each acquisition trial day, rats had four consecutive tests (60 s each) to find the hidden platform. If the platform was not found, rats were guided to the platform, removed after 10 s and placed in a holding cage with a 10 min intertrial interval. The entry quadrant was balanced within trials and across days. On Day 7, the platform was removed and rats were given a single 60 s extinction trial. The following day, the platform was placed in the diagonal quadrant and rats were given two reversal trials per day for 2 days. The location of the platform during acquisition and reversal was balanced across cohorts. At 16 month of age, 8 weeks after viral injection, the DREADD-expressing cohort was tested in the Morris water maze as described above, except that rats were pretreated with CNO (3 mg/kg i.p., NIDA Drug Supply Program; wild-type $n = 7$, TgF344-AD $n = 6$) or vehicle (5% DMSO in saline; wild-type $n = 9$,

TgF344-AD $n = 7$) 15 min prior to testing each day, and reversal learning testing was extended from 2 to 4 days.

Several days after completion of the Morris water maze, DREADD-expressing rats were injected with the same treatments they received in the Morris water maze (vehicle or CNO; 3 mg/kg i.p.) and perfused 105 min later to assess DREADD-induced c-Fos activation.

Data analysis

Data are reported as mean ± standard error, and the threshold for statistical significance was set at $\alpha = 0.05$. Statistical analysis was performed with SPSS, and graphs were generated by Graphpad Prism (La Jolla, CA) software. A two-way ANOVA was used to examine the effect of age and genotype for all immunohistochemistry and norepinephrine tissue level experiments, with Tukey's *post hoc* tests where appropriate. Stereology and locus coeruleus neuron culture values were compared using unpaired *t*-tests. For Morris water maze experiments, acquisition and reversal trials were analysed via separate repeated measures two-way ANOVAs. A three-way repeated measures ANOVA was used to examine acquisition and reversal trials in the DREADD Morris water maze cohort.

Results

TgF344-AD rats accumulate hyperphosphorylated tau in the locus coeruleus before the medial entorhinal cortex or hippocampus

Hyperphosphorylated tau accumulation in the locus coeruleus is the first sign of Alzheimer's disease-like pathology in humans, but has not been reported in amyloid-based transgenic rodent models of the disease (Braak *et al.*, 2011; Ehrenberg *et al.*, 2017). We found that 6-month- and 16-month-old TgF344-AD rats had hyperphosphorylated tau accumulation (CP13$^+$ cells) in the locus coeruleus, while wild-type littermates had little to no staining [$F(1,12) = 31.36$, $P = 0.0001$] (Fig. 1A and C). Moreover, there was a significant genotype × age interaction [$F(1,12) = 6.056$, $P = 0.03$]. A *post hoc* analysis showed that 16-month-old TgF344-AD rats had a significant, 2-fold increase in hyperphosphorylated tau$^+$ cells compared to 6-month-old transgenic animals. No significant staining was observed with any of the other tau antibodies (PHF-1, MC1) or stain (ThioS) examined, suggesting that tau filaments or fibrils have not formed in the locus coeruleus of the TgF344-AD rats by 16 months (data not shown). Similarly, the locus coeruleus was devoid of any amyloid-β staining by the 4G8 antibody at 16 months (data not shown).

The emergence of pretangle tau pathology follows a stereotyped pattern in Alzheimer's disease and is first detectable in the locus coeruleus (Braak 0), followed by the entorhinal cortex (Braak I) and the hippocampus (Braak II). As discussed above, TgF344-AD rats show hyperphosphorylated tau accumulation in the locus coeruleus at 6 months of age. However, tau pathology was not detected in the mEC or hippocampus until 16 months (Fig. 1B). A two-way ANOVA revealed a genotype × age interaction [mEC: $F(1,11) = 8.49$, $P = 0.01$; hippocampus: $F(1,11) = 11.9$, $P = 0.005$], and *post hoc* analysis showed significantly more CP13$^+$ cells in the 16 month TgF344-AD rats than wild-type littermates or 6 month TgF344-AD rats (Fig. 1D and E). TgF344-AD rats showed age-dependent accumulation of amyloid-β plaques in the mEC [$t(9) = 4.38$, $P = 0.002$] and hippocampus [$t(9) = 3.92$, $P = 0.004$] starting at 6 months, while no plaques were detected in wild-type rats regardless of age (Fig. 1F–H).

Because neuroinflammation is a hallmark of Alzheimer's disease and occurs in the hippocampus of TgF344-AD rats, we examined whether gliosis occurred in concert with hyperphosphorylated tau in the locus coeruleus. Overall, TgF344-AD rats showed elevated activated microglia (Iba1$^+$ cells) in the locus coeruleus compared to wild-type rats [$F(1,19) = 15.88$, $P = 0.0008$] (Fig. 2A and C), with the greatest genotype differences seen at 6 months. There was also an age-dependent reduction in activated microglia [$F(1,19) = 21.21$, $P = 0.0002$] with a borderline significant genotype × age interaction [$F(1,19) = 4.28$, $P = 0.05$]. Similar levels of astrocytes (GFAP$^+$ cells) were found in the locus coeruleus of wild-type and TgF344-AD rats [genotype: $F(1,12) = 0.22$, $P = 0.64$], with greater staining at 16 months [$F(1,12) = 5.62$, $P = 0.03$] (Fig. 2B and D). There was no genotype × age interaction for astrocyte number [$F(1,12) = 0.004$, $P = 0.95$].

Progressive noradrenergic fibre loss without locus coeruleus neuron death in TgF344-AD rats

Tau and neuroinflammation can be toxic to neurons, and the locus coeruleus degenerates in Alzheimer's disease. Thus, we examined whether locus coeruleus degeneration accompanied the pretangle tau and Iba-1 staining in TgF344-AD rats. At 16 months, unbiased stereology revealed no genotype differences in locus coeruleus neuron number [wild-type: 3502 ± 315; TgF344-AD: 3449 ± 282; $t(8) = 0.07$, $P = 0.90$], and locus coeruleus neuron volume was nearly identical between wild-type (1510 ± 128 μm^3) and TgF344-AD rats (1490 ± 195 μm^3) [$t(8) = 0.06$, $P = 0.96$]. We next examined locus coeruleus fibre density in the mEC, the next brain region to show tau pathology after the locus coeruleus in Alzheimer's disease. NET$^+$ fibres were significantly reduced in TgF344-AD rats compared to wild-type [$F(1,15) = 4.98$, $P = 0.04$] without a significant effect of age [$F(1,15) = 1.73$, $P = 0.21$] or a genotype × age interaction [$F(1,15) = 0.14$, $P = 0.72$] (Fig. 3A). Notably, hyperphosphorylated tau accumulation in locus coeruleus neurons was negatively correlated with locus coeruleus fibre density in the mEC [Pearson's $r = -0.55$, $P = 0.33$], suggesting that pretangle tau in the locus coeruleus may adversely impact neuron health and/or axonal stability (Fig. 3B).

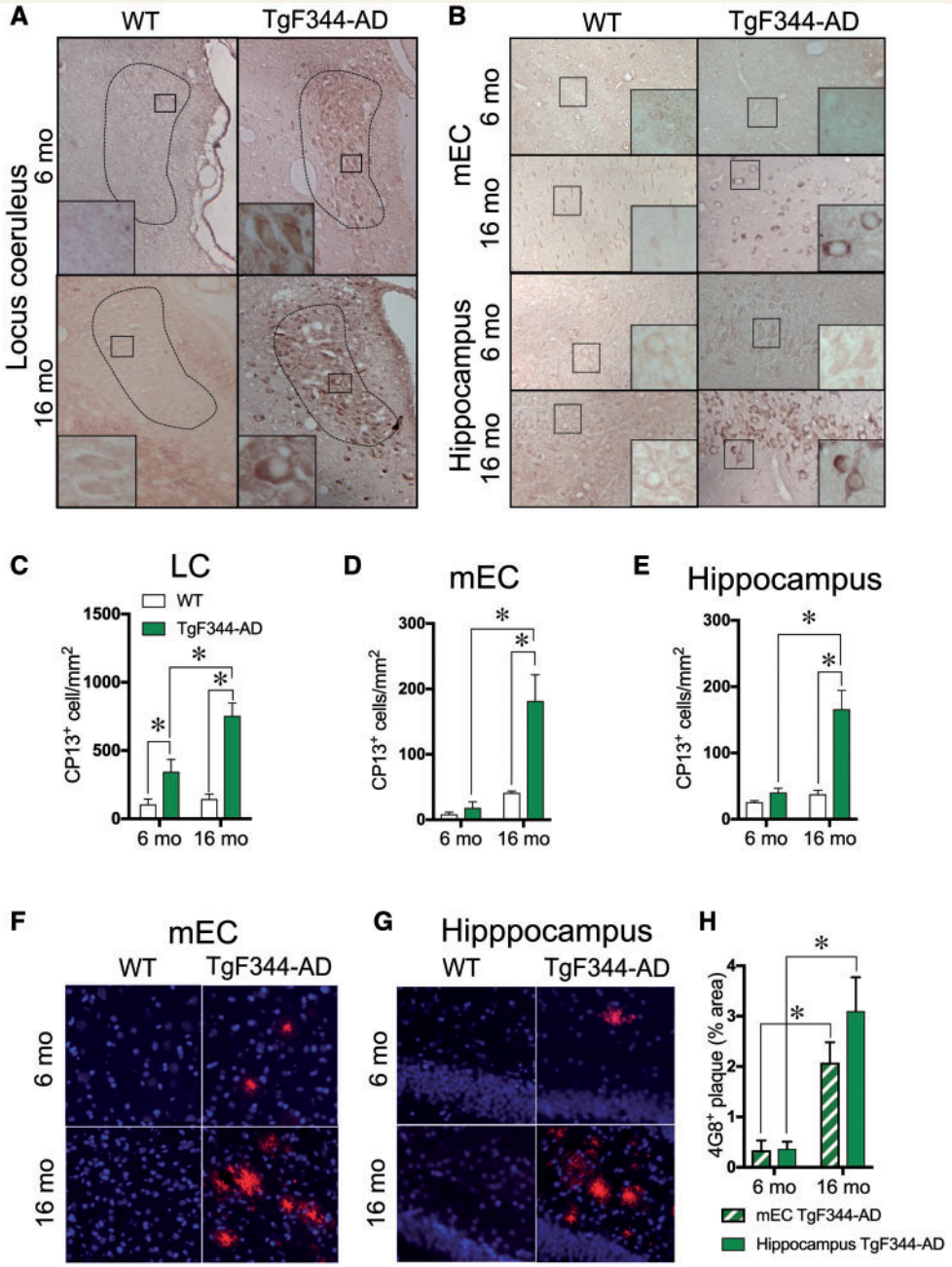

Figure 1 Pretangle tau immunoreactivity is detected in the locus coeruleus before the entorhinal cortex or hippocampus in TgF344-AD rats. Representative image (× 1, inset × 40) of hyperphosphorylated tau (CP13) of 6 month (n = 5/genotype) and 16 month (n = 5/genotype) wild-type and TgF344-AD rats in the locus coeruleus (**A**) and mEC and hippocampus (**B**). Quantification of CP13$^+$ cells in the locus coeruleus (**C**), mEC (**D**) and hippocampus (**E**) of wild-type (white bars) and TgF344-AD (green bars) rats. Representative images of amyloid-β accumulation (4G8; red) and Nissl (blue) in the mEC (**F**) and hippocampus (**G**) of 6-month and 16-month-old wild-type and TgF344-AD rats. Quantification of 4G8 plague burden in the mEC (striped green bars) and hippocampus (solid green bars) of TgF344-AD rats (**H**). *$P < 0.05$.

We extended these findings to investigate additional locus coeruleus-innervated regions affected in Alzheimer's disease. DBH$^+$ fibre density in the dentate gyrus revealed a significant genotype × age interaction [$F(1,22) = 5.78$, $P = 0.025$], and *post hoc* analysis showed that 16-month-old TgF344-AD rats had substantially reduced DBH$^+$ fibre density compared to 6-month-old TgF344-AD and 16-month-old wild-type rats (Fig. 3C and D). There were no significant interactions for any other subregion of the hippocampus [CA1: $F(1,22) = 0.28$, $P = 0.060$; CA3: $F(1,22) = 0.21$, $P = 0.65$; CA2: $F(1,22) = 0.51$, $P = 0.48$] nor was there a main effect of genotype [dentate gyrus: $F(1,22) = 3.49$,

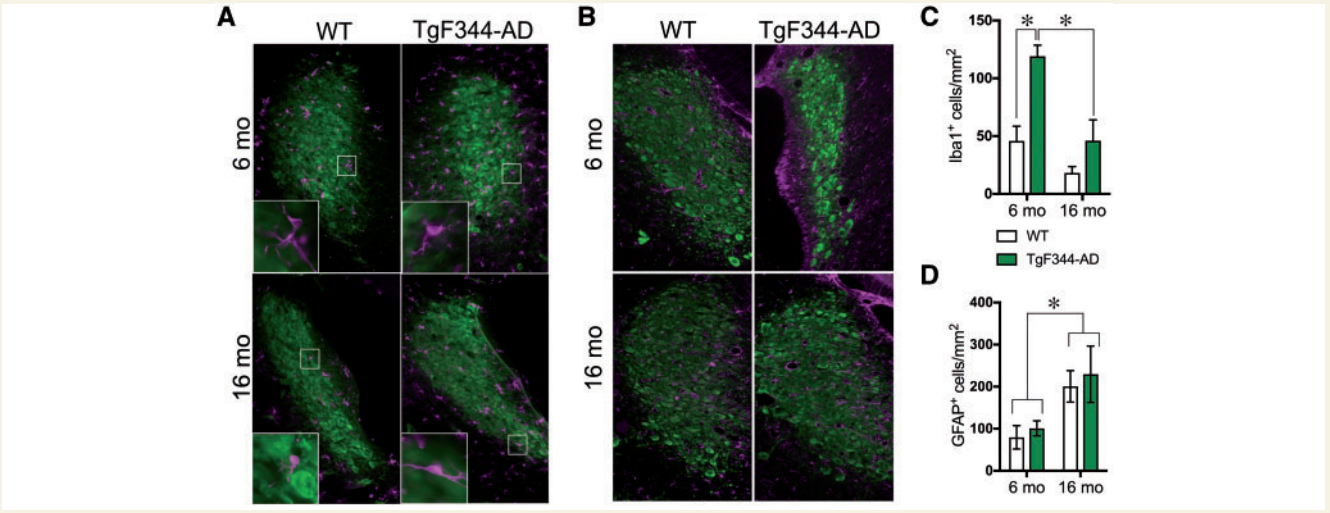

Figure 2 TgF344-AD rats show age-dependent alterations in glial cells in the locus coeruleus. Representative images of microglia (Iba1$^+$; magenta) (**A**) and activated astrocytes (GFAP$^+$; magenta) (**B**) in the locus coeruleus (TH$^+$; green) of 6 month (n = 5–6/genotype) and 16 month (6/genotype) wild-type and TgF344-AD rats. Quantification of Iba1$^+$ (**C**) and GFAP$^+$ cells (**D**) in the locus coeruleus of wild-type (open bars) and TgF344-AD (green bars) rats. *$P < 0.05$.

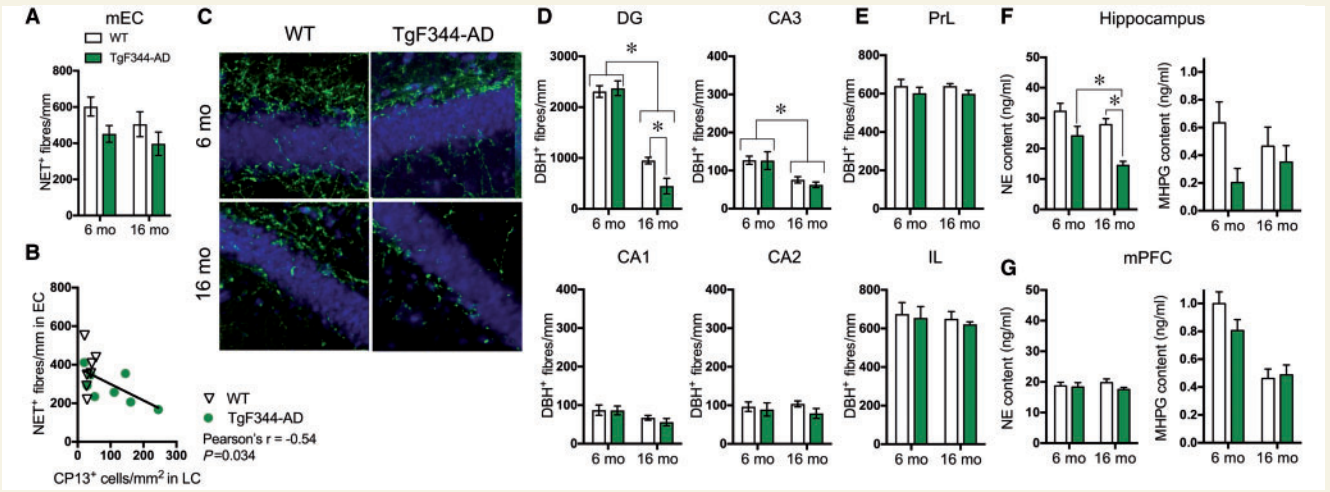

Figure 3 Region-specific progressive loss of locus coeruleus innervation and norepinephrine levels in TgF344-AD rats. Quantification of NET$^+$ fibre density in the mEC of 6 month (n = 4/genotype) and 16 month (n = 5/genotype) wild-type (open bars) and TgF344-AD rats (green bars) (**A**). Correlation between CP13 accumulation in locus coeruleus (LC) neurons and locus coeruleus innervation in the mEC in wild-type (open triangles) and TgF344-AD (green circles) (**B**). Representative images ($\times$40) of DBH$^+$ fibre (green) and Nissl (blue) staining in the dentate gyrus in wild-type and TgF344-AD rats (**C**). Quantification of DBH$^+$ fibre density in subregions of the hippocampus [dentate gyrus (DG), CA1, CA2, CA3] (**D**) and mPFC (IL = infralimbic: PrL = prelimbic) (**E**) of 6 month (n = 6/genotype) and 16 month (n = 7–8/genotype) wild-type and TgF344-AD rats. Norepinephrine (NE) and MHPG levels in hippocampus (**F**) and mPFC (**G**) tissue in 6 month (n = 6/genotype) and 16 month (n = 6/genotype) wild-type and TgF344-AD rats. *$P < 0.05$.

$P = 0.08$; CA1, $F(1,22) = 0.35$, $P = 0.56$; CA3: $F(1,22) = 0.29$, $P = 0.59$; CA2: $F(1,22) = 1.67$, $P = 0.21$] (Fig. 3D), although TgF344-AD DBH+ fibre density tended to be lower in all subregions at 16 months. In agreement with the literature (Ishida *et al.*, 2001), age-dependent reductions in DBH+ fibres were observed in the dentate gyrus [$F(1,22) = 195.0$, $P < 0.0001$], CA1 [$F(1,22) = 6.192$, $P = 0.02$] and CA3 regions [$F(1,22) = 18.63$, $P = 0.0003$], but not CA2 [$F(1,22) = 0.01$, $P = 0.91$] (Fig. 3D).

Similar to the mPFC norepinephrine levels, the prelimbic (PrL) and infralimbic (IL) cortices had similar DBH$^+$ fibre density across genotypes [PrL: $F(1,19) = 2.36$, $P = 0.14$; IL: $F(1,19) = 0.29$, $P = 0.60$] and age groups [PrL: $F(1,19) = 0.001$, $P = 0.97$; IL: $F(1,19) = 0.42$, $P = 0.53$] without a

significant genotype × age interaction [PrL: $F(1,21) = 0.15$, $P = 0.70$; IL: $F(1,19) = 0.001$, $P = 0.92$] (Fig. 3E). To examine whether other brain noradrenergic systems were also degenerating in TgF344-AD rats, DBH^+ fibre density was examined in the PVT, which receives innervation primarily from the A5 noradrenergic cell group rather than the locus coeruleus (Byrum and Guyenet, 1987). There was no effect of genotype [$F(1,19) = 0.13$, $P = 0.73$], age [$F(1,19) = 0.64$, $P = 0.44$] or genotype × age interaction [$F(1,19) = 0.19$, $P = 0.89$] (data not shown).

As an additional indication of locus coeruleus function, we examined tissue levels of norepinephrine and its metabolite MHPG in the in the hippocampus and mPFC using HPLC. At 6 months of age, there was a trend towards reduced norepinephrine and norepinephrine turnover (as measured by MHPG) in the hippocampus of TgF344-AD rats (Fig. 3F). By 16 months, TgF344-AD rats had a 48% decrease in hippocampal norepinephrine levels compared to wild-type littermates [$F(1,22) = 26.52$, $P < 0.0001$] (Fig. 3F). There was a significant age-dependent decrease in tissue norepinephrine levels [$F(1,22) = 11.38$, $P = 0.003$], resulting in a 40% reduction between 6-month- and 16-month-old TgF344-AD rats, but no genotype × age interaction [$F(1,22) = 1.63$, $P = 0.22$]. Overall, TgF344-AD rats also had significantly less hippocampal MHPG compared to wild-type rats [$F(1,22) = 4.33$, $P = 0.049$], but no age-dependent decline [$F(1,22) = 0.004$, $P = 0.95$] or genotype × age interaction [$F(1,22) = 0.98$, $P = 0.33$] (Fig. 3F). In the mPFC, norepinephrine levels were similar across genotypes [$F(1,24) = 1.25$, $P = 0.27$] and age groups [$F(1,24) = 0.02$, $P = 0.90$] without a genotype × age interaction [$F(1,24) = 0.65$, $P = 0.43$] (Fig. 3G). In the mPFC, MHPG levels showed a marked age-dependent [$F(1,24) = 31.53$, $P < 0.0001$] reduction regardless of genotype [$F(1,24) = 1.22$, $P = 0.28$], with no genotype × age interaction [$F(1,24) = 2.06$, $P = 0.16$] (Fig. 3G). Thus, similar to clinical mild cognitive impairment/early Alzheimer's disease, TgF344-AD rats displayed locus coeruleus axon/terminal degeneration and dysfunction in the absence of cell body loss (Chan-Palay and Asan, 1989; Booze *et al.*, 1993; Kori *et al.*, 2016; Theofilas *et al.*, 2017). These noradrenergic deficits were preferentially found in the mEC and hippocampus.

Aggregate-prone mutant tau expression reduces locus coeruleus neurite length *in vitro*

Tau is a microtubule-stabilizing protein, and its hyperphosphorylation leads to axonal instability, suggesting that pretangle tau accumulation in the locus coeruleus may contribute to the loss of locus coeruleus innervation (Khan and Bloom, 2016). To determine whether the presence of aberrant tau is sufficient to impair locus coeruleus neuron structure, we examined locus coeruleus neuron morphology and survival in primary cultures derived from TH-GFP mice with or without P301S tau (Fig. 4A). P301S tau transgenic mice develop $CP13^+$ hyperphosphorylated tau pathology that is very similar to what we observed in the TgF344-AD rats (Allen *et al.*, 2002; Xu *et al.*, 2014). Locus coeruleus neurite length was reduced by 69% in cultures derived from TH-GFP/P301S mice compared to TH-GFP alone [$t(12) = 3.94$, $P = 0.029$] (Fig. 4B and C), but there was no difference in locus coeruleus neuron survival [$t(12) = 0.48$, $P = 0.63$] (Fig. 4D). These data are consistent with the idea that aberrant tau contributes to the loss of locus coeruleus axons/terminals in TgF344-AD rats and in prodromal Alzheimer's disease.

Spatial reversal learning is impaired in TgF344-AD rats

Locus coeruleus activity and adrenergic receptor signalling in the hippocampus contribute to spatial learning, and 16-month-old TgF344-AD rats have modest deficits

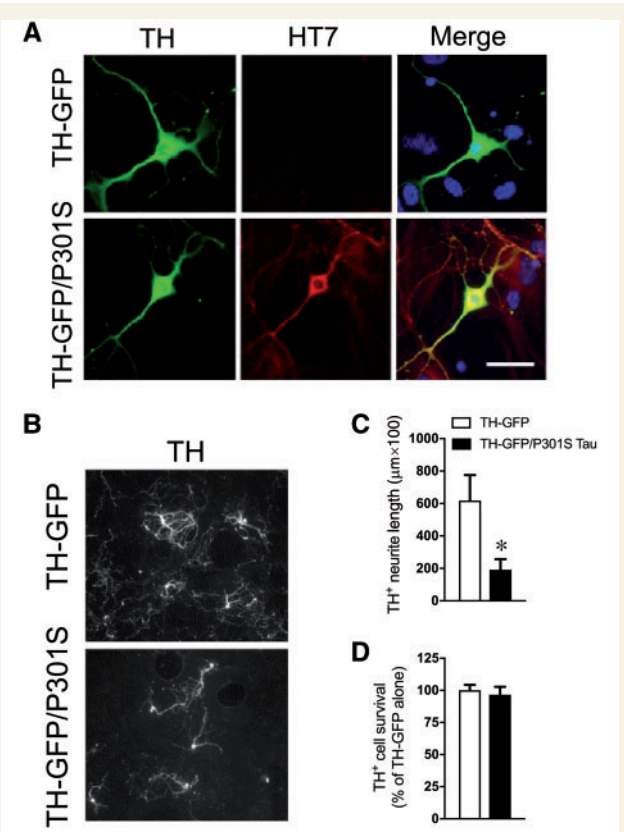

Figure 4 Expression of mutant tau reduces locus coeruleus neurite length *in vitro*. Representative images (× 40) of human tau (HT7; red) in cultured locus coeruleus (TH^+; green) neurons from TH-GFP and TH-GFP/P301S mice (**A**). Representative images (× 20) of mature (DIV 11) locus coeruleus neurons (TH^+; white) in cultures from TH-GFP ($n = 5$) and TH-GFP/P301S ($n = 8$) mice (**B**). Quantification of locus coeruleus neurite length (**C**) and cell survival (**D**) in TH-GFP (open bars) and TH-GFP/P301S (filled bars) cultures. *$P < 0.05$.

during initial learning and more severe abnormalities during reversal learning in the Barnes maze (Cohen *et al.*, 2013; Hagena *et al.*, 2016). We examined spatial memory deficits using the Morris water maze, a hippocampus-dependent task that is modulated by noradrenergic transmission. During acquisition trials, both age groups were able to learn the task, as indicated by decreased latency to find the hidden platform across trials [6 months: $F(5,50) = 21.12$, $P < 0$ 0.0001; 16 months: $F(5,50) = 16.50$, $P < 0.0001$] (Fig. 5A). A significant genotype × trial interaction for latency at 6 months [$F(5,50) = 2.66$, $P = 0.033$] and 16 months revealed a modest deficit in TgF344-AD rats [$F(5,50) = 2.7$, $P = 0.031$]. *Post hoc* analysis indicated that the TgF344-AD rats took longer to find the platform on Day 1 in 6-month-old rats (Fig. 5A) and on Day 5 in 16-month-old rats (Fig. 5C). There was a genotype effect on latency at 6 months [$F(1,10) = 7.06$, $P = 0.02$], with a trend at 16 months [$F(1,10) = 3.26$, $P = 0.10$] Differences in latency were not due to swim speed, which was similar across genotypes at both ages [6 months: $F(1,10) = 2.75$, $P = 0.13$; 16 months: $F(1,10) = 0.68$, $P = 0.43$] (Fig. 5B and D).

During reversal trials, TgF344-AD rats took longer to find the new platform location than did wild-type rats in the 6 month [$F(1,10) = 21.64$, $P < 0.0009$] (Fig. 5A) and 16 month [$F(1,10) = 6.25$, $P = 0.03$] (Fig. 5C) cohorts, while swim speeds were similar between genotypes [6 months: $F(1,10) = 3.86$, $P = 0.08$; 16 months: $F(1,10) = 0.02$, $P = 0.89$] (Fig. 5B and D). There were no genotype × trial interactions in 6-month-old [latency: $F(1,10) = 0.001$, $P = 0.98$; $P = 0.90$; speed: $F(1,10) = 0.71$, $P = 0.42$] or 16-month-old rats [latency: $F(1,10) = 0.001$, $P = 0.93$; speed: $F(1,10) = 0.87$, $P = 0.37$]. There was no correlation between DBH^+ fibre density in the hippocampus and performance in acquisition or reversal trials in the Morris water maze in 16-month-old rats [Pearson's r = 0.15, $P = 0.56$].

DREADD-induced locus coeruleus activation restores reversal learning to TgF344-AD rats in the Morris water maze

DREADDs have been used to selectively activate locus coeruleus neurons and modulate rodent behaviour (Vazey and Aston-Jones, 2014; Fortress *et al.*, 2015), and we wished to examine their ability to rescue cognitive impairment in TgF344-AD rats. An AAV containing the excitatory hM3Dq DREADD with an HA tag under control of the PRSx8 promoter was delivered stereotaxically into the locus coeruleus of 13.5-month-old wild-type and TgF344-AD rats, which resulted in robust locus coeruleus-specific DREADD expression (Fig. 6A). To assess the capability of locus coeruleus activation to rescue learning and memory deficits, 16-month-old wild-type and TgF344-AD rats expressing hM3Dq in the locus coeruleus were injected with

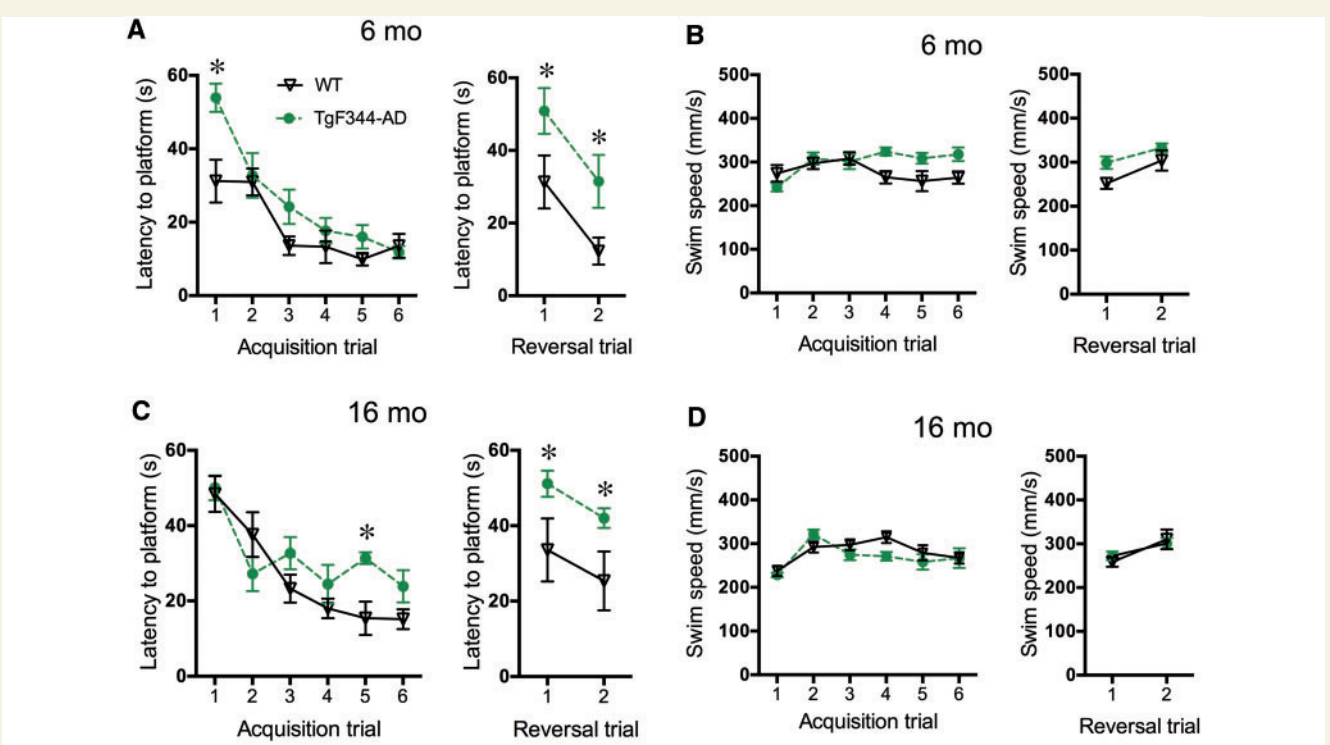

Figure 5 Spatial reversal learning is impaired in TgF344-AD rats. Latency to the platform during acquisition and reversal trials of the Morris water maze in 6 month (n = 6/genotype) (**A**) and 16 month (n = 6/genotype) (**C**) wild-type (black triangles) and TgF344-AD (green circles) rats. Swim speed during Morris water maze trials in 6 month (**B**) and 16 month (**D**) rats. *$P < 0.05$.

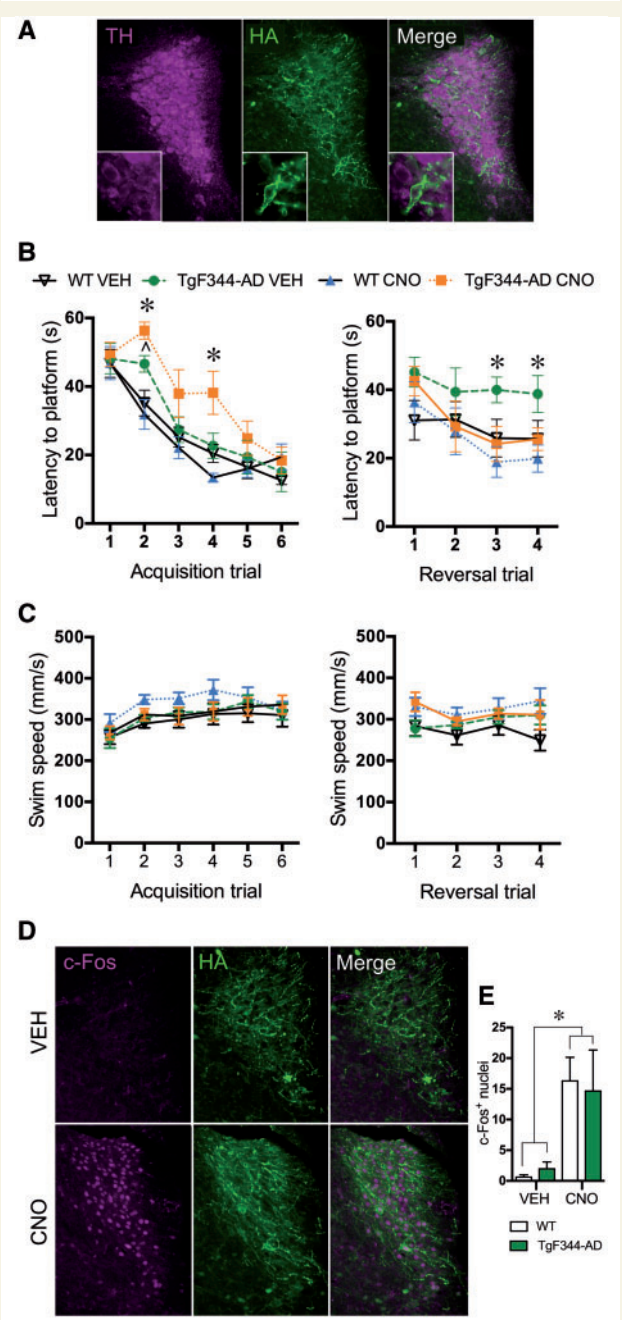

Figure 6 DREADD-induced locus coeruleus activation restores reversal learning in TgF344-AD rats. Representative image (× 10, inset × 40) of PRSx8-HA-hM3Dq DREADD (HA tag; green) expression in locus coeruleus neurons (TH^+; magenta) (**A**). Latency to the platform during acquisition and reversal trials of the Morris water maze following vehicle (VEH) or CNO (3 mg/kg i.p.) pretreatment in wild-type (n = 7–9/treatment group) and TgF344-AD (n = 6–7/treatment group) rats (**B**). Swim speed during Morris water maze trials (**C**). Representative images (× 10) of c-Fos (magenta) in the locus coeruleus (TH^+; green) of DREADD-expressing rats following vehicle (VEH) or CNO (3 mg/kg i.p.) administration (**D**). Quantification of c-Fos^+ nuclei in the locus coeruleus of DREADD-expressing wild-type (open bars) and TgF344-AD (green bars) rats following vehicle or CNO administration (**E**). *$P < 0.05$ for TgF344-AD CNO versus wild-type vehicle and TgF344-AD vehicle, ^$P < 0.05$ for TgF344-AD vehicle versus wild-type vehicle.

vehicle or CNO (3 mg/kg i.p.) 30 min prior to each Morris water maze trial. During acquisition, all groups significantly decreased latency over days [$F(5,125) = 49.65$, $P < 0.0001$] (Fig. 6B). There was a significant genotype × drug × trial interaction [$F(3,25) = 6.63$, $P = 0.002$], and *post hoc* analysis showed that CNO-pretreated TgF344-AD rats were initially slower to find the platform compared to CNO-pretreated wild-type and vehicle-pretreated TgF344-AD rats. In addition, vehicle-pretreated TgF344-AD rats were initially slower to find the platform than their wild-type counterparts. However, by Trial 5, latencies were indistinguishable between groups, indicating similar acquisition learning. There were no differences in swim speed [genotype: $F(1,27) = 0.14$, $P = 0.71$; treatment: $F(1,27) = 2.45$, $P = 0.13$; interaction: $F(3,24) = 0.87$, $P = 0.47$] (Fig. 6C).

We next examined the effects of locus coeruleus activation on reversal learning. Latency to the platform showed a significant genotype × drug × trial effect [$F(3,25) = 4.65$, $P = 0.01$]. Similar to our data with surgically-naïve rats, *post hoc* analysis showed that TgF344-AD rats pretreated with vehicle took longer to find the platform than wild-type counterparts on reversal trials 3 and 4 (Fig. 6B). CNO had no effect on the performance of wild-type rats, but restored normal reversal learning in TgF344-AD rats (Fig. 6B). CNO-pretreated TgF344-AD rats found the platform faster than vehicle-pretreated TgF344-AD on Day 3 with a trend for Day 4 ($P = 0.08$), and their latency was not different than wild-type rats, regardless of pretreatment. Swim speed was similar across groups [$F(3,25) = 1.99$, $P = 0.14$] (Fig. 6C).

To confirm that DREADDs were able to activate locus coeruleus neurons, rats were injected with vehicle or CNO (3 mg/kg i.p.) several days after completing the Morris water maze, and euthanized 105 min later. Brain slices containing the locus coeruleus were examined for the expression of the DREADD and the immediate early gene c-Fos, a marker of neuronal activity. CNO significantly increased c-Fos^+ nuclei in the locus coeruleus [$F(1,18) = 12.26$, $P = 0.003$] to a similar degree in both genotypes (Fig. 6D and E), indicating successful and equivalent locus coeruleus activation in wild-type and TgF344-AD rats.

Discussion

Clinical evidence suggests that aberrant tau accumulation in the locus coeruleus and noradrenergic dysfunction may be a critical early step in Alzheimer's disease progression (Chalermpalanupap *et al.*, 2013; Mather and Harley, 2016). Yet, an accurate preclinical model of these phenotypes does not exist, hampering the identification of underlying mechanisms and the development of locus coeruleus-based therapies. Current models are unsuitable because amyloid-based mouse models do not manifest tau pathology in the locus coeruleus, and neurotoxic lesions of the locus coeruleus produce catastrophic loss of cell

bodies not observed in humans until late in the disease (Theofilas *et al.*, 2017; Kelly *et al.*, 2017). Based on our present findings, the TgF344-AD rat uniquely meets the criteria for a suitable model of early locus coeruleus dysfunction in Alzheimer's disease (Fig. 7). Namely, these animals displayed endogenous hyperphosphorylated tau in the locus coeruleus prior to tau pathology in the mEC or hippocampus. This locus coeruleus pathology was correlated with decreased locus coeruleus innervation in the mEC. Additionally, TgF344-AD rats had reduced locus coeruleus fibre density in the dentate gyrus and norepinephrine levels in the hippocampus. These changes occurred without frank locus coeruleus neuron degeneration, which would be more reminiscent of mid- to late-stage Alzheimer's disease. Locus coeruleus deficits were accompanied by impaired reversal learning in the Morris water maze, a hippocampus-dependent task that is influenced by the locus coeruleus/norepinephrine system. Importantly, DREADD-induced locus coeruleus activation restored normal reversal learning to aged TgF344-AD rats, indicating that enhancing locus coeruleus tone can improve cognition, even in the context of an ailing locus coeruleus and forebrain amyloid-β and tau pathology.

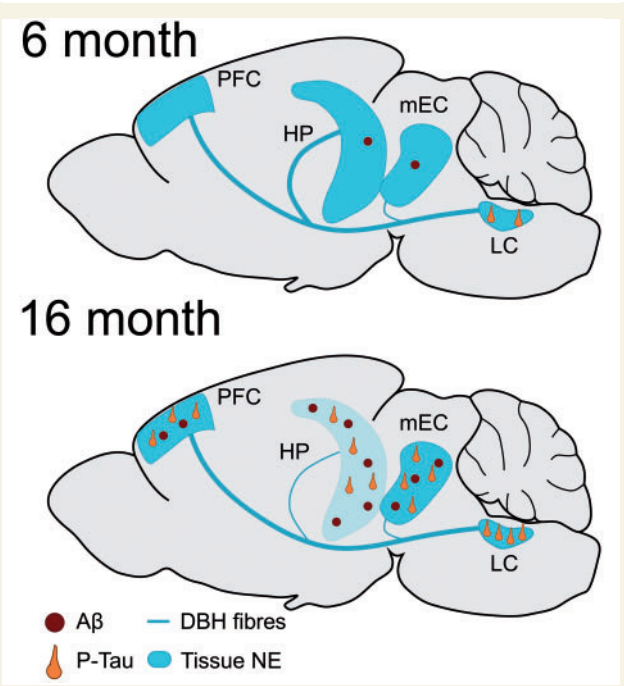

Figure 7 Overview of tau and amyloid-β pathology in the TgF344-AD rats. At 6 months, the locus coeruleus is the only brain region of TgF344-AD rats that shows pretangle tau accumulation (orange neurons), while the mEC and hippocampus (HP) contain low levels of amyloid-β (Aβ) deposition (red circles). Tau and amyloid-β pathologies are detectable across the brain (with the exception of amyloid-β in the locus coeruleus) at 16 months. Reductions in locus coeruleus innervation (blue line) begin in the mEC at 6 months of age. At 16 months, decreased locus coeruleus innervation and norepinephrine (NE) levels (blue colour) are evident in the hippocampus but not PFC of TgF344-AD rats.

Hyperphosphorylated tau accrual in the locus coeruleus is one of the first detectable signs of Alzheimer's disease neuropathology in the brain, appearing decades prior to cognitive impairment (Braak and Del Tredici, 2012). Similarly, age-dependent hyperphosphorylated tau immunoreactivity was found in the locus coeruleus of TgF344-AD rats, which do not express human tau transgenes, making these rats the only Alzheimer's disease model encompassing endogenous tauopathy in the locus coeruleus. The most robust staining in the locus coeruleus was observed with the CP13 antibody, a marker of nascent tau hyperphosphorylation (Augustinack *et al.*, 2002). Little staining was observed with the PHF-1 or MC1 antibodies or ThioS stain, which detect more advanced stages of tau hyperphosphorylation or protein aggregation, respectively (Augustinack *et al.*, 2002). Although TgF344-AD rats accumulated aberrant tau in the locus coeruleus, this did not coincide with locus coeruleus neuron loss. Likewise, pretangle tau can be detected in the locus coeruleus of Alzheimer's disease patients years before the typical onset of cell body degeneration (Theofilas *et al.*, 2017; Ehrenberg *et al.*, 2017).

Hyperphosphorylated tau in TgF344-AD rats approximates Braak staging and was observed in the locus coeruleus before tau pathology in the mEC or hippocampus (Braak *et al.*, 2011; Cohen *et al.*, 2013; Ehrenberg *et al.*, 2017). Importantly, these results replicate previous work showing emergence of tau pathology in the hippocampus and PFC of TgF344-AD rats at 16 month of age (Cohen *et al.*, 2013). Wild-type rats also showed low levels of CP13 staining in the locus coeruleus, mEC and hippocampus, which might indicate small amounts of hyperphosphorylated tau but more likely reflects non-specific staining, which is common with phosphorylation-dependent tau antibodies (Petry *et al.*, 2014). Combined, these results suggest that tau hyperphosphorylation emerges and progresses in the locus coeruleus of TgF344-AD rats prior to other brain regions, similar to prodromal Alzheimer's disease.

Previous work has shown robust amyloid-β deposition in the hippocampus and PFC in the TgF344-AD rats at 16 months of age (Cohen *et al.*, 2013). Despite a ubiquitous prion promoter driving the APP/PS1 transgene, amyloid-β pathology was excluded from the locus coeruleus of TgF344-AD rats, which aligns with Braak's failure to detect amyloid-β in the locus coeruleus (Braak *et al.*, 2011). Contrary to the initial description of TgF344-AD rats, we observed low levels of amyloid-β in the mEC and hippocampus at 6 months, indicating that pretangle tau is not the only Alzheimer's disease-like pathology present relatively early in these animals. Additional research is necessary to investigate the exact timing and pattern of aberrant tau and amyloid-β emergence in TgF344-AD rats.

Although there was no overt locus coeruleus neuron loss in the TgF344-AD rats, locus coeruleus dysfunction was

evident. In the mEC, TgF344-AD rats had slight drop in locus coeruleus innervation compared to wild-type rats, yet more striking was the negative correlation between pretangle tau accumulation in the locus coeruleus and locus coeruleus fibre density. This result is consistent with the reduced norepinephrine levels observed in the entorhinal cortex of rabbits with aluminum-induced neurofibrillary tangles (Beal *et al.*, 1989). Notably, norepinephrine hyperpolarizes entorhinal cortex neurons, and thus decreased locus coeruleus innervation may lead to disinhibition and hyperexcitability in the dentate gyrus, a feature of early Alzheimer's disease (Xiao *et al*, 2009; Yassa *et al.*, 2010).

Abnormally low levels of forebrain norepinephrine have been reported in Alzheimer's disease (Chalermpalanupap *et al.*, 2013). Modest reductions in norepinephrine and MPHG, a norepinephrine metabolite, were observed in the hippocampus of 6-month-old TgF344-AD rats compared to wild-type littermates, and these differences became stark at 16 months. In the older cohort, the reduced norepinephrine levels coincided with diminished locus coeruleus fibre density in the dentate gyrus. Compared to other hippocampus subregions, the dentate gyrus has the greatest density of locus coeruleus fibres and is most sensitive to age-dependent synapse loss; thus it makes intuitive sense that the largest reductions were observed here (Small *et al.*, 2004; Amaral *et al.*, 2007). In addition, tau pathology in the dentate gyrus is negatively correlated with onset and severity of clinical dementia in patients with Alzheimer's disease (Seifan *et al.*, 2015). Likewise, decreased density and morphological changes in locus coeruleus fibres and alterations in adrenergic receptors are found in patients with Alzheimer's disease (Chan-Palay and Asan, 1989; Booze *et al.*, 1993; Szot, 2006). Surprisingly, reductions in noradrenergic fibre density and norepinephrine levels were not observed in the mPFC, indicating that dysfunction was not universal across brain regions innervated by the locus coeruleus. The locus coeruleus sends collateralized projections, with a single neuron branching widely throughout the brain, suggesting that selective fibre loss may be due, in part, to regional differences in the terminal field environment (Schwarz *et al.*, 2015; Kebschull *et al.*, 2016).

In humans with Alzheimer's disease, tau pathology in the locus coeruleus and noradrenergic dysfunction are associated, but it is not known whether the accumulation of aberrant tau 'causes' the observed reductions in locus coeruleus fibres and norepinephrine levels in the forebrain. To determine the functional consequences of pathogenic tau, we examined the survival and morphology of cultured locus coeruleus neurons from transgenic mice expressing P301S tau, a mutant form of human tau that is prone to hyperphosphorylation and aggregation and produces CP13$^+$ pathology that is very similar to what we observed in the TgF344-AD rats (Allen *et al.*, 2002; Xu *et al.*, 2014). We found that locus coeruleus neurons from P301S tau mice had shorter neurites than neurons from control littermates, indicating that aberrant tau is capable of damaging locus coeruleus neurons. Future studies will be required to identify the cellular mechanisms underlying tau-induced locus coeruleus neurite dysmorphology, but we note that hyperphosphorylated tau has reduced affinity for microtubules, which can result in microtubule instability and negatively impact outgrowth (Khan and Bloom, 2016). Likewise, retinal cultures from P301S mice show reduced axonal outgrowth in response to neurogenerative stimuli compared to wild-type mice, suggesting outgrowth may be affect by tau (Gasparini *et al.*, 2011). No effect was observed on locus coeruleus survival, and TgF344-AD rats displayed no locus coeruleus cell body loss up to 16 months of age. These results are reminiscent of human Alzheimer's disease, where hyperphosphorylated tau persists in locus coeruleus neurons for years before frank degeneration occurs (Andres-Benito *et al.*, 2017; Ehrenberg *et al.*, 2017). If aberrant tau is responsible for locus coeruleus neuron death in Alzheimer's disease, its actions are slow and/or require additional insults.

Forebrain neuroinflammation is a hallmark of many neurodegenerative diseases; however, few studies have investigated inflammation in the locus coeruleus (Heneka *et al.*, 2015). In rats, human tau increases the expression of inflammatory cytokines in the locus coeruleus, and chronic administration of lipopolysaccharide increases microglial infiltration and degeneration (Bardou *et al.*, 2014; Mravec *et al.*, 2016). Pretangle tau, microglia and locus coeruleus degeneration are found in patients with more advanced Alzheimer's disease, after Braak stage III (Andres-Benito *et al.*, 2017; Ehrenberg *et al.*, 2017; Kelly *et al.*, 2017). We detected increased microglia in the locus coeruleus region of 6-month-old TgF344-AD rats compared to wild-type animals, a time that coincides with the appearance of pretangle tau in the locus coeruleus and the beginning signs of noradrenergic dysfunction in the hippocampus. It is not clear whether the presence of hyperphosphorylated tau triggers the neuroinflammation, or whether an initial inflammatory environment promotes the aberrant tau accumulation. Unexpectedly, Iba-1$^+$ microglia decreased with age in the rat locus coeruleus, regardless of genotype. While the exact cause for this age-dependent drop is unknown, normal ageing reduces microglia process length, resulting in reduced and non-uniform coverage within the cortex (Baron *et al.*, 2014). Thus, it is possible that the change in Iba-1 staining in the locus coeruleus reflects decreased microglial process coverage. In addition, there are regional differences in microglia density and sensitivity to age-dependent changes throughout the brain (Hart *et al.*, 2012*)*, which may explain the differences between the hippocampus (Cohen *et al.*, 2013), which shows increases in Iba-1 staining with age, and locus coeruleus of the TgF344-AD rats. Stereologic and morphologic analysis is necessary to further examine and characterize microglia within the locus coeruleus. Nevertheless, TgF344-AD rats display age-dependent histological and neurochemical evidence of diminished locus coeruleus function that closely mimics the status of the locus coeruleus in

mild cognitive impairment/early Alzheimer's disease, providing an ideal platform to test noradrenergic therapies that target the long clinical window that exists while the locus coeruleus is impaired but before it is devastated.

Contextual and spatial learning are corrupted in Alzheimer's disease, and modulated by locus coeruleus activity and norepinephrine transmission (Hagena *et al.*, 2016). Notably, spatial reversal learning depends on long term depression within the hippocampus, and locus coeruleus electrical stimulation can induce long term depression in the dentate gyrus (Hansen and Manahan-Vaughan, 2015*b*). We found that deficits in spatial reversal learning were evident in TgF344-AD rats at 6 months and worsened over time in concordance with locus coeruleus dysfunction. By contrast, TgF344-AD rats showed only modest deficits during acquisition training. Poor Morris water maze acquisition is observed following manipulations that eliminate locus coeruleus/norepinephrine function, while comparatively minor disruptions of locus coeruleus/norepinephrine function have no effect on acquisition of this task but do impair reversal learning (Heneka, 2006; Khakpour-Taleghani *et al.*, 2009; Jardanhazi-Kurutz *et al.*, 2010; Fentress *et al.*, 2013; Hammerschmidt *et al.*, 2013; Kummer *et al.*, 2014; Coradazzi *et al.*, 2016). Factors besides noradrenergic deficits may be contributing to cognitive impairment in this model. amyloid-β deposition, tau pathology, apoptotic neuron loss and gliosis are present in the hippocampus of 16-month-old TgF344-AD animals, and intra-hippocampal infusion of amyloid-β impairs reversal learning but not acquisition in rats (Cohen *et al.*, 2013; Scuderi *et al.*, 2014).

Previous studies have shown that locus coeruleus lesions exacerbate cognitive deficits in APP transgenic mouse models of Alzheimer's disease, while enhancement of norepinephrine transmission via increasing norepinephrine synthesis or inhibiting reuptake can ameliorate these deficits (Jardanhazi-Kurutz *et al.*, 2010; Kalinin *et al.*, 2012; Hammerschmidt *et al.*, 2013; Kummer *et al.*, 2014; Totah *et al.*, 2015). Locus coeruleus stimulation or pharmacological increases in norepinephrine levels enhance performance in spatial learning and reversal learning in a spatial set-shifting paradigm, respectively (Hansen and Manahan-Vaughan, 2015*a*; Totah *et al.*, 2015). We took a chemogenetic approach to determining whether locus coeruleus activation could enhance cognition in our model, which has several advantages. First, to our knowledge, the TgF344-AD rat is the only model of Alzheimer's disease that displays endogenous tau pathology in the locus coeruleus and accompanying locus coeruleus dysfunction reminiscent of mild cognitive impairment/early Alzheimer's disease. This is an important point, since any therapy directed at a clinical population would, by definition, occur in the context of impaired locus coeruleus function. Second, while conventional pharmacological approaches (e.g. systemic administration of a norepinephrine reuptake blocker or adrenergic receptor agonist) alter all central and peripheral norepinephrine signalling and may produce unwanted cardiovascular and other side effects, viral delivery of DREADDs allows the specific manipulation of locus coeruleus-derived norepinephrine transmission. We found that DREADD-induced locus coeruleus activation restored normal reversal learning in the Morris water maze in 16-month-old TgF344-AD rats. Based on the importance of the hippocampus for reversal learning and the noradrenergic deficits there in the TgF344-AD rats, we suspect that increased norepinephrine transmission in this brain region was responsible for the improved cognition. However, the locus coeruleus also sends broad projections to the forebrain, so it is possible that alternative circuits are mediating this effect, and future experiments using site-specific infusions of CNO will be necessary to delineate the critical neuroanatomical substrates.

Although DREADD-induced locus coeruleus activation clearly improved reversal learning, it also increased latency during early acquisition trials in the TgF344-AD rats. Locus coeruleus neurons fire in two distinct modes: tonic activity, which is associated with behavioural flexibility, distractibility, and anxiety; and phasic activity, which is associated with goal-directed behaviour and increased task performance (Sara, 2009). The hM3Dq DREADD appears to selectively increase tonic locus coeruleus firing (Vazey and Aston-Jones, 2014), which may improve reversal learning via enhanced behavioural flexibility, but slightly impair acquisition due to distractibility and anxiety (McCall *et al.*, 2015). Future experiments using optogenetics, which can drive either tonic or phasic locus coeruleus firing, will be useful for distinguishing these possibilities. DREADD activation had no effect during acquisition or reversal trials in wild-type rats, presumably because these animals have intact locus coeruleus systems that are already functioning optimally. Similarly, DREADD-induced locus coeruleus activation restored working memory in a transgenic mouse model of Down syndrome that displays locus coeruleus degeneration, but had no effect in wild-type controls (Fortress *et al.*, 2015).

The present results suggest that locus coeruleus/norepinephrine-based therapeutics may provide cognitive enhancement in mild cognitive impairment/early Alzheimer's disease. Currently, there are several FDA-approved noradrenergic drugs for treatment of other neurological/neuropsychiatric disorders that are safe in the elderly, thus paving the way for accelerated clinical implementation (Chalermpalanupap *et al.*, 2013). Of note, atomoxetine, a selective norepinephrine transporter inhibitor prescribed for attention deficit and hyperactivity disorder, enhances norepinephrine transmission and cognitive performance in humans (Ince Tasdelen *et al.*, 2015). Although atomoxetine was an ineffective treatment for individuals with mid- to late-stage Alzheimer's disease (Mohs *et al.*, 2009), it is likely that frank locus coeruleus and hippocampus degeneration had already occurred in these patients, robbing atomoxetine of viable noradrenergic synapses to modulate. The drug is currently in a phase II clinical trial for individuals with mild cognitive impairment (NCT01522404). In addition, the synthetic norepinephrine precursor L-3,4-dihydroxyphenylerine (L-DOPS;

droxidopa) has been used as an adjunct therapy for Parkinson's disease, a disorder where locus coeruleus neuron degeneration also occurs, and an atomoxetine + L-DOPS cocktail rescued learning and memory deficits in the 5xFAD transgenic mouse model (Kalinin *et al.*, 2012; Hale *et al.*, 2017). Thus, droxidopa may also have medicinal potential in Alzheimer's disease.

Conclusion

As Alzheimer's disease research turns towards earlier detection and intervention, it is critical to have accurate preclinical models in order to probe disease mechanisms and test the efficacy of novel therapeutics. The TgF344-AD rat uniquely recapitulates many aspects of locus coeruleus dysfunction observed in early Alzheimer's disease, especially pertaining to pretangle tau accumulation, local neuroinflammation, and reductions in hippocampal noradrenergic fibres and norepinephrine levels. Hyperphosphorylated tau in the locus coeruleus is the first detectable Alzheimer's disease-like pathology in the brain, but locus coeruleus neurons do not die until mid-stage disease, indicating that a considerable window for intervention exists. Our finding that DREADD-induced locus coeruleus activation rescues cognitive deficits in TgF344-AD rats at a time when the locus coeruleus is already compromised and other Alzheimer's disease-like neuropathology has infiltrated the forebrain bodes well for locus coeruleus/norepinephrine-based therapeutics.

Acknowledgements

We thank C. Strauss, L. Walker, and A. Levey for helpful editing of the manuscript, L. Walker for technical advice, Brice Bowerman for help with colony management, and E. Vazey and G. Aston-Jones for providing some of the PRSX8-hM3Dq-HA virus.

Funding

This work was supported the National Institutes of Health (AG0476670 to D.W. and RMC, NS007480 to J.M.R.) and the Alzheimer's Association (IIRG-13-278692 to D.W.).

References

Allen B, Ingram M, Takao M, Smith MJ, Jakes R, Virdee K et al. Abundant tau filaments and nonapoptotic neurodegeneration in transgenic mice expressing human P301S tau protein. J Neurosci 2002; 22: 9340–51.

Alzheimer's Association. 2016 Alzheimer's disease facts and figures. Alzheimers Dement 2016; 12: 459–509.

Amaral DG, Scharfman HE, Lavenex P. The dentate gyrus: fundamental neuroanatomical organization (dentate gyrus for dummies). Prog Brain Res 2007; 163: 3–22.

Andres-Benito P, Fernandez-Duenas V, Margarita MC, Escobar LA, Torrejon-Escribano B, Aso E, et al. Locus coeruleus at asymptomatic early and middle Braak stages of neurofibrillary tangle pathology. Neuropathol Appl Neurobiol 2017; 38: 42–9.

Aston-Jones G, Cohen JD. An integrative theory of locus coeruleus-norepinephrine function: adaptive gain and optimal performance. Annu Rev Neurosci 2014; 28: 403–50.

Augustinack JC, Schneider A, Mandelkow EM, Hyman BT. Specific tau phosphorylation sites correlate with severity of neuronal cytopathology in Alzheimer's disease. Acta Neuropathol 2002; 103: 26–35.

Bardou I, Kaercher RM, Brothers HM, Hopp SC, Royer S, Wenk GL. Age and duration of inflammatory environment differentially affect the neuroimmune response and catecholamine neurons in the midbrain and brainstem. Neurobiol Aging 2014; 35: 1065–73.

Baron R, Babcock AA, Nemirovsky A, Finsen B, Monsonego A. Accelerated microglia pathology is associated with amyloid beta plaques in mouse model of Alzheimer's disease. Aging Cell 2014; 13: 584–95.

Booze RM, Mactutus CF, Gutman CR, David JN. Frequency analysis of catecholamine axonal morphology in human brain. J Neurol Sci 1993; 119: 110–18.

Braak H, Del Tredici K. Where, when, and in what form does sporadic Alzheimer's disease begin? Curr Opin Neurol 2012; 25: 708–14.

Braak H, Thal DR, Ghebremedhin E, Tredici KD. Stages of the pathologic process in Alzheimer disease: age categories From 1 to 100 Years. J Neuropathol Exp Neurol 2011; 70: 960–9.

Beal MF, Mazurek MF, Ellison DW, Kowall NM, Solomon PR, Pendelbury WW. Neurochemical characteristics of aluminium-induced neurofibrillary degeneration in rabbits. Neuroscience 1989; 29: 339–46.

Byrum CE, Guyenet PG. Afferent and efferent connections of the A5 noradrengergic cell group in the rat. J Comp Neurol 1987; 261: 529–42.

Chalermpalanupap T, Kinkead B, Hu WT, Kummer MP, Hammerschmidt T, Heneka MT, et al. Targeting norepinephrine in mild cognitive impairment and Alzheimer's disease. Alzheimers Res Ther 2013; 5: 21.

Chan-Palay V, Asan E. Alterations in catecholamine neurons of the locus coeruleus in senile dementia of the Alzheimer's type and Parkinson's disease with and without dementia and depression. J Comp Neurol 1989; 287: 373–92.

Cohen RM, Rezai-Zadeh K, Weitz TM, Rentsendorj A, Gate D, Spivak I, et al. A Transgenic Alzheimer rat with plaques, tau pathology, behavioral impairment, oligomeric Aβ , and frank neuronal loss. J Neurosci 2013; 33: 6245–56.

Coradazzi M, Gulino R, Fieramosca F, Falzacappa LV, Riggi M, Leanza G. Selective noradrenaline depletion impairs working memory and hippocampal neurogenesis. Neurobiol Aging 2016; 48: 93–102.

Do Carmo S, Cuello AC. Modeling Alzheimer's disease in transgenic rats. Mol Neurodegener 2013; 8: 37.

Ehrenberg AJ, Nguy A, Theofilas P, Dunlop S, Suemoto CK, Di Lorenzo Alho AT, et al. Quantifying the accretion of hyperphosphorylated tau in the locus coeruleus and dorsal raphe nucleus: the pathological building blocks of early Alzheimer's disease. Neuropathol Appl Neurobiol 2017; 43: 393–408.

Feinstein D, Kalinin S, Braun D. Causes, consequences, and cures for neuroinflammation mediated via the locus coeruleus. J Neurochem 2016; 139: 154–78.

Fentress HM, Klar R, Krueger JJ, Sabb T, Redmon SN, Wallace NM, et al. Norepinephrine transporter heterozygous knockout mice exhibit altered transport and behavior. Genes Brain Behav 2013; 12: 749–59.

Fortress AM, Hamlett ED, Vazey EM, Aston-Jones G, Cass WA, Boger HA, et al. Designer receptors enhance memory in a mouse model of down syndrome. J Neurosci 2015; 35: 1343–53.

Gasparini L, Crowther RA, Martin KR, Berg N, Coleman M, Goedert M, Spillantini MG. Tau inclusions in retinal ganglion cells of human P301S tau transgenic mice: effects on axonal viability. Neurol Aging 2011; 32: 419–33.

Gundersen H, Jensen E, Kieu K, Nielsen J. The efficiency of systematic sampling in stereology – reconsidered. J Microscop 1999; 193: 199–211.

Hagena H, Hansen N, Manahan-Vaughan D. β-Adrenergic control of hippocampal function: subserving the choreography of synaptic information storage and memory. Cereb Cortex 2016; 26: 1349–64.

Haglund M, Sjöbeck M, Englund E. Locus ceruleus degeneration is ubiquitous in Alzheimer's disease: possible implications for diagnosis and treatment. Neuropathology 2006; 26: 528–32.

Hale GM, Valdes J, Brenner M. A review of the treatment of primary orthostatic hypotension. Ann of Pharmacother 2017; 51: 417–28.

Hammerschmidt T, Kummer MP, Terwel D, Martinez A, Gorji A, Pape HC, et al. Selective loss of noradrenaline exacerbates early cognitive dysfunction and synaptic deficits in APP/PS1 mice. Biol Psychiatry 2013; 73: 454–63.

Hansen N, Manahan-Vaughan D. Hippocampal long-term potentiation that is elicited by perforant path stimulation or that occurs in conjunction with spatial learning is tightly controlled by beta-adrenoreceptors and the locus coeruleus. Hippocampus 2015a; 25: 1285–98.

Hansen N, Manahan-Vaughan D. Locus coeruleus stimulation facilitates long-term depression in the dentate gyrus that requires activation of β-adrenergic receptors. Cereb Cortex 2015b; 25: 1889–96.

Hart AD, Wyttenback A, Perry VH, Teeling JL. Age related changes in microglia phenotype vary between CNS region: grey versus white matter differences. Brain Behav Immun 2012; 5: 754–65.

Heneka MT, Carson MJ, Khoury JE, Landreth G, Brosseron F, Feinstein D, et al. Neuroinflammation in Alzheimer's disease. Lancet Neurol 2015; 14: 388–405.

Heneka MT, Galae E, Gavriluyk V, Dumitrescu-Ozimek L, Daeschner J, O'Banion MK, et al. Noradrenergic depletion potentiates beta amyloid-induced cortical inflammation. J Neurosci 2002; 22: 2434–42.

Heneka MT. Locus coeruleus degeneration promotes Alzheimer pathogenesis in amyloid precursor protein 23 transgenic mice. J Neurosci 2006; 26: 1343–54.

Ince Tasdelen B, Karakaya E, Oztop DB. Effects of atomoxetine and osmotic release oral system-methylphenidate on executive functions in patients with combined type attention-deficit/hyperactivity disorder. J Child Adolesc Psychopharmacol 2015; 25: 494–500.

Ishida Y, Shirokawa T, Miyaishi O, Komatsu Y. Age-dependent changes in noradrenergic innervations of the frontal cortex in F344 rats. Neurobiol Aging 2001; 22: 283–6.

Jardanhazi-Kurutz D, Kummer MP, Terwel D, Vogel K, Dyrks T, Thiele A, et al. Induced LC degeneration in APP/PS1 transgenic mice accelerates early cerebral amyloidosis and cognitive deficits. Neurochem Int 2010; 57: 375–82.

McCall JG, Al-Hasani R, Siuda ER, Hong DY, Norris AJ, Ford CP, et al. CRH engagement of the locus coeruleus noradrenergic system mediates stress-Induced Anxiety. Neuron 2015; 87: 605–20.

Kalinin S, Polak PE, Lin SX, Sakharkar AJ, Pandey SC, Feinstein DL. The noradrenaline precursor L-DOPS reduces pathology in a mouse model of Alzheimer's disease. Neurobiol Aging 2012; 33: 1651–63.

Kebschull JM, da Silva PG, Reid AP, Peikon ID, Albeanu DF, Zador AM. High-throughput mapping of single-neuron projections by sequencing of barcoded RNA. Neuron 2016; 91: 975–87.

Kelly SC, He B, Perez SE, Ginsberg SD, Mufson EJ, Counts SE. Locus coeruleus cellular and molecular pathology during the progression of Alzheimer's disease. Acta Neuropathol Commun 2017; 5: 8.

Khakpour-Taleghani B, Lashgari R, Motamedi F, Naghdi N. Effect of reversible inactivation of locus coeruleus on spatial reference and working memory. Neuroscience 2009; 158: 1284–91.

Khan SS, Bloom GS. Tau: the center of a signaling nexus in Alzheimer's disease. Front Neurosci 2016; 10: 2474.

Kori M, Aydın B, Unal S, Arga KY, Kazan D. Metabolic biomarkers and neurodegeneration: a pathway enrichment analysis of Alzheimer's disease, Parkinson's disease, and Amyotrophic Lateral Sclerosis. OMICS 2016; 20: 645–61.

Kummer MP, Hammerschmidt T, Martinez A, Terwel D, Eichele G, Witten A, et al. Ear2 deletion causes early memory and learning deficits in APP/PS1 mice. J Neurosci 2014; 34: 8845–54.

Mather M, Harley CW. The locus coeruleus: essential for maintaining cognitive function and the aging brain. Trends Cogn Sci 2016; 20: 214–26.

Mohs RC, Shiovitz TM, Tariot PN, Porsteinsson AP, Baker KD, Feldman PD. Atomoxetine augmentation of cholinesterase inhibitor therapy in patients with Alzheimer disease: 6-month, randomized, double-blind, placebo-controlled, parallel-trial study. Am J Geriatr Psychiatry 2009; 17: 752–759.

Morrissette DA, Parachikova A, Green KN, LaFerla FM. Relevance of transgenic mouse models to human Alzheimer disease. J Biol Chem 2009; 284: 6033–7.

Mravec B, Lejavova K, Vargovic P, Ondicova K, Horvathova L, Novak P, et al. Tauopathy in transgenic (SHR72) rats impairs function of central noradrenergic system and promotes neuroinflammation. J Neuroinflammation 2016; 13: 15.

Petry FR, Pelletier J, Bretteville A, Morin F, Calon F, Herbert SS et al. Specificity of anti-tau antibodies when analyzing mice models of Alzheimer's disease: problems and solutions. PLoS One 2014; 9: e94251.

Sara SJ. The locus coeruleus and noradrenergicmodulation of cognition. Nat Rev Neurosci 2009; 10: 211–23.

Sathyanesan A, Ogura T, Lin W. Automated measurement of nerve fiber density using line intensity scan analysis. J Neurosci Methods 2012; 206: 165–75.

Schwarz LA, Miyamichi K, Gao XJ, Beier KT, Weissbourd B, DeLoach KE, et al. Viral-genetic tracing of the input–output organization of a central noradrenaline circuit. Nature 2015; 524: 88–92.

Scuderi C, Stecca C, Valenza M, Ratano P, Bronzuoli MR, Bartoli S, et al. Palmitoylethanolamide controls reactive gliosis and exerts neuroprotective functions in a rat model of Alzheimer's disease. Cell Death Dis 2014; 5: e1419–12.

Seifan A, Marder KS, Mez J, Noble JM, Cortes EP, Vonsattel JP, et al. Hippocampal laminar distribution of tau relates to Alzheimer's disease and age of onset. J Alzheimers Dis 2015; 43: 315–24.

Small SA, Chawla MK, Buonocore M, Rapp PR, Barnes C. Imaging correlates of brain function in monkeys and rats isolates a hippocampal subregion differentially vulnerable to aging. Proc Natl Acad Sci USA 2004; 101: 7181–6.

Song, CH, Fan X, Exeter CJ, Hess EJ, Jinnah HA. Functional analysis of dopaminergic systems in a DYT1 knock-in mouse model of dystonia. Neurobiol Dis 2012; 48: 66–78.

Szot P. Compensatory changes in the noradrenergic nervous system in the locus coeruleus and hippocampus of postmortem subjects with Alzheimer's disease and dementia with Lewy bodies. J Neurosci 2006; 26: 467–78.

Theofilas P, Ehrenberg AJ, Dunlop S, Di Lorenzo Alho AT, Nguy A, Leite RE, et al. Locus coeruleus volume and cell population changes during Alzheimer's disease progression: a stereological study in human postmortem brains with potential implication for early-stage biomarker discovery. Alzheimers Dement 2017; 13: 236–46.

Tomlinson BE, Irving D, Blessed G. Cell loss in the locus coeruleus in senile dementia of Alzheimer's type. J Neurol Sci 1981; 49: 419–28.

Totah NK, Logothetis NK, Eschenko O. Atomoxetine accelerates attentional set shifting without affecting learning rate in the rat. Psychopharmacology 2015; 232: 3697–707.

Turnbull MT, Coulson EJ. Cholinergic basal forebrain lesion decreases neurotrophin signaling without affecting tau hyperphosphorylation in genetically susceptible mice. J Alzheimers Dis 2017; 55: 1141–54.

Vazey EM, Aston-Jones G. Designer receptor manipulations reveal a role of the locus coeruleus noradrenergic system in isoflurane general anesthesia. Proc Natl Acad Sci USA 2014; 111: 3859–64.

Wilson RS, Nag S, Boyle PA, Hizel LP, Yu L, Buchman AS, et al. Neural reserve, neuronal density in the locus ceruleus, and cognitive decline. Neurology 2013; 80: 1202–8.

Weinshenker D. Functional consequences of locus coeruleus degeneration in Alzheimer's disease. Curr Alzheimer Res 2008; 5: 342–5.

Woerman AL, Aoygai A, Patel S, Kazmi SA, Lobach I, Grinber LT, et al. Tau prions from Alzheimer's disease and chronic traumatic encephalopathy patients propagate in cultured cells. Proc Nat Acad Sci USA 2016; 113: E8187–96.

Xiao Z, Deng PY, Rojanathammanee L, Yang C, Grisanti L, Permpoonputtana K, et al. Noradrenergic depression of neuronal excitability in the entorhinal cortex via activation of TREK-2 K+ channels. J Biol Chem 2009; 284: 10980–91.

Xu H, Rolser TW, Carlsson T, de Andrade A, Bruch J, Hollerhage M et al. Memory deficits correlate with tau and spine pathology in P301S MAPT transgenic mice. Neuropathol Appl Neurobiol 2014; 7: 833–43.

Yassa MA, Stark SM, Bakker A, Albert MS, Gallagher M, Stark CE. High-resolution structural and functional MRI of hippocampal CA3 and dentate gyrus in patients with amnestic Mild Cognitive Impairment. Neuroimage 2010; 15: 1242–52.